

Magnetic fields in GRBs

Maxim Lyutikov

Abstract

We discuss the dynamical role of magnetic fields in GRB explosions in the framework of the fireball and electromagnetic models. We contrast the observational predictions of the two models and argue that only the very early afterglow observations, almost coincident with the prompt phase, can be used as decisive tests of the ejecta content.

1 Introduction

One of the key issues in GRBs physics is whether magnetic fields play an important dynamical role at any stage in the outflow. Currently, the overwhelming point of view, advocated by the fireball model (FBM) is that magnetic fields do not play any major dynamical role. In the frame work of the FBM magnetic field are small scale, with correlation length l_c much smaller than the "horizon" length $l_c \ll R/\Gamma$ (R is the radius of the outflow in the laboratory frame and Γ is a bulk Lorentz factor). Small scale magnetic fields can be created locally in the flow; once created their energy density falls off faster with radius than plasma energy density, so that they do not affect the overall dynamics of the outflow.

Alternative approach, advocated by MHD and electromagnetic models (*e.g.* Lyutikov & Blandford, 2003) is that there are dynamically important large scale fields with "super-horizon" correlation length $l_c \geq R/\Gamma$. Such magnetic fields must be created at the source; at large distances the toroidal component of the field dominates; it's energy density $B_\phi^2 \propto r^{-2}$ scales similar to plasma energy density $\rho c^2 \propto r^{-2}$ (for spherical outflow; pressure falls off faster), so that they potentially can be important (or even dominate) for the overall dynamics of the flow. To quantify the dynamical importance of large scale magnetic fields, it is useful to introduce magnetization parameter σ as a ratio of Poynting F_{Poynting} to (cold) particle F_p fluxes

$$\sigma = \frac{F_{\text{Poynting}}}{F_p} = \frac{B^2}{4\pi\Gamma\rho c^2} = \frac{b'^2}{8\pi\rho'c^2} \quad (1)$$

where B and ρ are magnetic field and plasma density in the lab frame, b' and ρ' are magnetic field and plasma density in the plasma frame (where electric field is zero). In the FBM $\sigma \ll 1$, MHD models work in the regime $\sigma \sim 1$, EMM model assumes $\sigma \gg 1$. The question of the GRB model is then reduced to the question how large is σ in the ejecta?

The current state of the GRB theory is such that too often all the results are interpreted in terms of FBM, so that any new discovery is seen as a confirmation of it, while alternative models are often called an extension of a FBM. In an effort to clear up the terminology we suggest the following definitions based on the energy content of the GRB ejecta (due to page constraints we limit our discussion to two models: fireball and electromagnetic). These two types of models are at the extreme limits of σ ; one may imagine an intermediate, MHD models with $\sigma \sim 1$.

Fireball model (FBM, *e.g.* Piran , 2004): The defining characteristic is that most energy produced by the central source is carried by the bulk motion of ions. In temporal order the transformations of energy are as follows. The initial source of energy is not specified. Initial energy is thermalized near the central source, so that most of it is converted into lepto-photonic plasma. This internal energy is then converted to the bulk motion of ions, and reconverted back into internal at internal shocks; at the same time, the small scale magnetic fields are generated. The energy of these generated magnetic fields is then used to accelerate leptons via Fermi mechanism to highly relativistic energies (note that the energy that goes to non-thermal particles is *electro-magnetic* even in the FBM: Fermi-type acceleration is done by turbulent EMF associated with fluctuations of magnetic field).

Electro-magnetic model, (EMM, *e.g.* Lyutikov & Blandford, 2003). The defining characteristic of the electro-magnetic model is that the bulk energy of the flow is carried by magnetic field. In temporal order the evolution of the energy proceeds as follows. The energy that will power a GRB comes from kinetic rotational energy of the central source (millisecond pulsar or BH-disk system). It is then converted to magnetic energy using unipolar inductor (like in pulsars), transported to large distances and is used to accelerate particle directly through reconnection-type events.

2 Large scale magnetic fields

Theoretically, large scale, energetically dominant magnetic fields are expected in the launching regions of relativistic outflows. This is exemplified by pulsars, which generate magnetized winds, and by AGN jets, launched and collimated by electromagnetic stresses (*e.g.* through Blandford-Znajek mechanism). Lat-

est full relativistic MHD numerical simulations of accretion on to black hole do show formation of the strongly-magnetized axial funnel McKinney & Gammie (2004).

3 Look early!

How can the two models be distinguished? Below we argue that only direct observations at the prompt phase and very early afterglows (AG) can be used to distinguish the model: observations of the late afterglows can be used only as hints at best.

AG evolution may be separated into two phases with very different dynamics which we will call early and late AG.

I. Early AG. In a FBM, the early AG phase is when the total swept-up mass is of the order of the eject mass $t \sim (E_\Omega/\Gamma_0^2\rho_{ISM}c^5)^{1/3}$ where E_Ω is the energy of explosion per unit solid angle, Γ_0 is initial Lorentz factor and t is coordinate time (we assume $\rho_{ISM} = constant$). At the early AG the Lorentz factor of the flow is constant. In EMM, the early AG is when the fast magneto-sonic waves emitted by the source are still catching with the surface of the expanding bubble. This stage ends at $t \sim (E_\Omega t_s/\Omega\Gamma_0^2\rho_{ISM}c^5)^{1/4}$ where $t_s \sim 30$ s is the source activity period (in observer time t_{ob} this stage ends when $t_{ob} \sim t_s$). At the early AG the Lorentz factor is decreasing $\Gamma \propto t^{-1/2}$ and is much higher than in the FBM.

II. Late AG. At the late AG stage, when most of the energy has been transferred to the forward shock, the system forgets (almost completely, see below) what was the content of the ejecta (*e.g.* ions or magnetic field); this stage is approximated by Blandford-McKee self-similar solution (*e.g.* , for constant outside density and in the non-radiative regime $\Gamma \propto r^{-3/2}$). *The overall temporal behavior of late AG is determined by the total energy release (and not the form of that energy) and, as a consequence, can hardly be used to distinguish between the models. On the other hand, early AG, which are virtually coincident with the prompt phase, have very different behavior and can be used to distinguish between the models.*

There are still *subtle* properties of late AGs that may serve as indications in favor of one or the other model. Beside the explosion energy, relativistic forward shock still "remembers" the angular distribution of the deposited energy $E(\theta)$. This "memory" comes, first, from the fact that two points on the shock wave front separated by the angle $\Delta\theta \geq 1/\Gamma$ are causally disconnected, and secondly, from relativistic kinematics freeze-out of forces normal to the shock front (*e.g.* Shapiro, 1979) even inside the cone $\Delta\theta \leq 1/\Gamma$. As a result, $E(\theta)$ remains approximately constant in time (ballistic expansion) until $\Gamma \sim$ several, after which point the non-spherical forward shock starts to evolve

laterally toward sphericity.¹

Thus, *the angular distribution of the total energy $E(\theta)$ can be used to distinguish between different models, if a model predicts it.* This can be related to the extensive discussion about the structure of the GRB outflows ("uniform jet" or "structured jet"), or, to be more precise, about the structure of the forward shock generated by the explosion. The implications of one or the other profile seem to be never mentioned. The FBM does not make any predictions for $E(\theta)$. The electromagnetic model, on the other hand, does predict $E(\theta) \propto 1/\theta^2$, the "structured jet".

Another possible hint from later AG may come from polarization measurements. If magnetic field is produced locally, the polarization fraction and the position angle must correlate with "jet break time" (for "uniform jets" polarization fraction goes through zero while the position angle experiences a 90° flip at the "jet break time"; for "structured jets" the polarization fraction peaks at the moment of "jet break" while the position angle remains constant). In the EMM, it is feasible that ejecta magnetic field mixes with the shocked plasma and provides a source of polarization. In this case the position angle remains constant through the AG, while the polarization fraction is constant before the "jet break" and decreases afterward Lazzati et al. (2004).

4 Tests of GRB models

Decisive tests of different GRB models are bound to come from observations (almost) contemporaneous with the prompt emission.

Reverse shock emission. Perhaps the simplest test of GRB models may come from observations of emission from the reverse shock propagating in the ejecta, which typically falls into the optical range. Note, that such a key observation that may validate a GRB theory may come from a small scale experiment, like ROTSE or RAPTOR. FBM predicts (modulo the adjustable parameters like the ratio of magnetic to plasma energy densities) strong reverse shock emission, so that absence of nearly contemporaneous optical emission in most GRBs is a strong argument against FBM (MHD modeling of reverse shock emission seem to favor high σ in the ejecta, Zhang & Kobayashi (2004)). In EMM reverse shock is absent (optical flash may be produced by other mechanisms, like gamma-ray pair production in front of the forward shock, Beloborodov (2004)).

¹ We would like to stress that at the late AG stage there no "jet", but a non-spherical shock wave evolving in time. The expressions like "jet break times", "jet sideways expansion" etc are all misnomers.

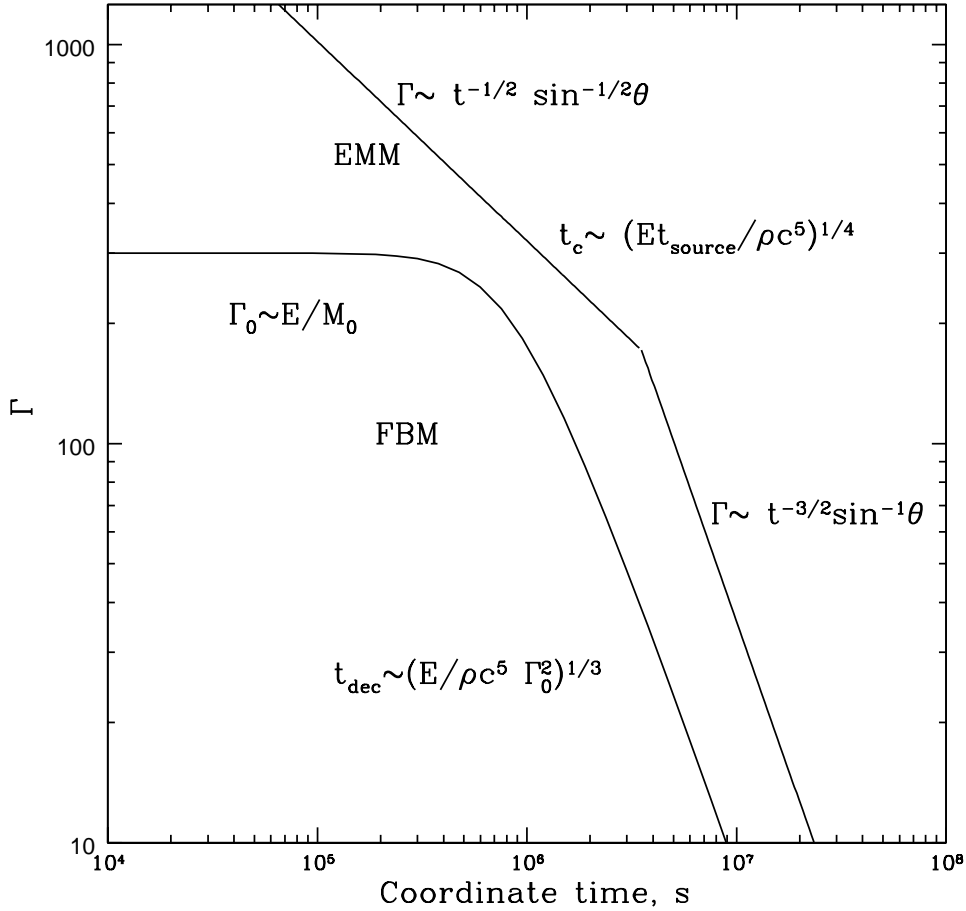


Fig. 1. Evolution of Lorentz factors in the FBM and EMM at early AG $t_{ob} \leq t_{GRB}$ for constant external density. Overall normalization of the curves depends on the viewing angle (in the EMM). Generally, at a given time the Lorentz factors in EMM are higher than in the FBM.

Spectra of early AGs. FBM and EMM make very different prediction for the properties of early AGs (see Fig 1). According to EMM, at the early AG stage the Lorentz factor and peak frequency are much larger (and falling with time) than in the FBM (constant Lorentz factor and peak frequency). Thus, early afterglow in the EMM are more energetic than in FBM and can blend with the prompt phase. Practically, the observations required to distinguish the models are tricky, both because of the tight temporal constraints, and because the early AG emission is faint: it increases as the burst progresses, reaching maximum at the end of prompt/early AG phase.

Polarization of prompt emission. Claims of high polarization Coburn & Boggs (2003), if confirmed, may provide a decisive test of GRB models. There is no question that the best way to produce polarization in the limit $10\% \leq \Pi \leq 60\%$ is through synchrotron emission in large scale magnetic fields Lyutikov et al.

	FBM		EMM	
	$\rho = const$	$\rho = \rho_0(r_0/r)^2$	$\rho = const$	$\rho = \rho_0(r_0/r)^2$
Lorentz factor Γ	$\frac{E_0 c^2}{M_0}$	$\frac{E_0 c^2}{M_0}$	$\left(\frac{L}{\rho c^5}\right)^{1/8} t_{ob}^{-1/4}$	$\left(\frac{L}{\rho_0 r_0^2 c^3}\right)^{1/4}$
Peak frequency ν_m	$\frac{m_p^2 e \sqrt{\rho}}{m_e^3} \Gamma_0^4 \epsilon_e^2 \epsilon_B^{1/2}$	$\sqrt{2\pi} \frac{m_p^2 e \sqrt{\rho_0}}{m_e^3 c} r_0 \Gamma_0^2 \epsilon_e^2 \epsilon_B^{1/2} t_{ob}^{-1}$	$\frac{m_p^2 e \sqrt{L}}{m_e^3 c^{5/2}} \epsilon_e^2 \epsilon_B^{1/2} t_{ob}^{-1}$	$\frac{m_p^2 e \sqrt{L}}{m_e^3 c^{5/2}} \epsilon_e^2 \epsilon_B^{1/2} t_{ob}^{-1}$
Peak flux $F_{nu,max}$	$\frac{e^3 c^2 \Gamma_0^8 \rho^{3/2}}{D^2 m_e^2 m_p} \epsilon_B^{1/2} t_{ob}^2$	$\frac{e^3 \Gamma_0^2 r_0^3 \rho_0^{3/2}}{m_e^2 m_p c D^2} \epsilon_B^{1/2}$	$\frac{e^3 L \sqrt{\epsilon_B} \sqrt{\rho}}{c^3 D^2 m_e^2 m_p} t_{ob}$	$\frac{e^3 \sqrt{L} r_0^2 \rho_0}{c^{5/2} m_e^2 m_p D^2} \epsilon_B^{1/2}$
Cooling frequency ν_c	$\frac{1}{64 \sqrt{2} \pi^{3/2}} \frac{m_e^5 c^6}{e^7 \Gamma_0^4 \epsilon_B^{3/2} \rho^{3/2}} t_{ob}^{-2}$	$\frac{c^9 m_e^5 \Gamma_0^2}{16 \sqrt{2} \pi^{3/2} e^7 r_0^3 \epsilon_B^{3/2}} t_{ob}$	$\frac{m_e^5 c^{17/2}}{e^7 \sqrt{L} \rho \epsilon_B^{3/2}} t_{ob}^{-1}$	$\frac{c^{15/2} m_e^5 \sqrt{L}}{8 \sqrt{2} \pi^{3/2} r_0^4 \epsilon_B^{3/2} \rho_0^2} t_{ob}$
End of early AG, t_{ob}	$\left(\frac{E_\Omega}{\Gamma_0^8 \rho c^5}\right)^{1/3}$	$\frac{E_\Omega}{2c^3 r_0^2 \Gamma_0^4 \rho_0}$	$t_s \sim t_{GRB}$	$t_s \sim t_{GRB}$

Table 1. Properties of early afterglows. Post-shock plasma is parametrized by ϵ_e , the ratio of electron energy density to total energy density, and ϵ_B , the ratio of magnetic field energy density to total. D is distance to the source.

(2003). (Larger polarization can only be produced with inverse Compton mechanism, smaller polarization can be produced by small scale magnetic fields.) The FBM need to make several independent assumptions and fine tuning of parameters in order to produce high polarization: (i) jet opening angle $\sim 1/\Gamma$, (ii) viewing angle $\sim 1/\Gamma$, (iii) small scatter of Lorentz factors (this runs contrary to the very basic assumption of the FBM!), (iv) nearly perfect alignment of all shocks' normals with radial direction *in the bulk frame*, (v) two-dimensional turbulent magnetic fields. In order to get polarization in double digits the FBM needs to fine tune all these factors independently.

Observational consequences of the EMM Observational properties of the EMM listed below follow from the assumption that the central source generates strongly magnetized wind with small baryon loading, and that the electrical current in the wind is concentrated near the axis:

- Weak thermal precursor. If a fraction $1/\sigma \sim 0.01 - 0.1$ of the magnetic energy is dissipated near the source, this should produce a thermal precursor with luminosity $\sim 0.01 - 0.1$ of the main GRB burst. FBM generally predict strong thermal precursor (*e.g.* Daigne and Mochkovitch, 2002).
- High polarization of prompt emission.
- Constant position angle of AG polarization along the projection of the axis on the plane of the sky (same position angle as in prompt if both are seen)
- Hard-to-soft spectral evolution (similar to "radius-to-frequency" mapping in pulsars). At later times emission is generated at larger radii, where magnetic field is lower.
- $\epsilon_{peak} \propto \sqrt{L_\Omega}$. In EMM, $B \sim \sqrt{L_\Omega}$ (since $L \sim B^2 r^2 c$); for synchrotron emission, the peak energy is proportional to magnetic field.
- No emission from the reverse shock. Strongly magnetized plasma supports only weak shocks, if at all.
- Decreasing peak frequency during early AG (for constant density surrounding).
- "Universal jet" structure of AG. Magnetically-dominated outflows have a preferred distribution of currents: when most of the current is concentrated near the axis of the flow Heyvaerts and Norman (2003) (this configuration corresponds to a minimum energy given total magnetic flux). In this case $B \sim 1/\sin \theta$ and $L_\Omega \sim 1/\sin^2 \theta$.
- AG peak flux reaches its maximum at the end of prompt phase (in FBM the moment of peak flux is not tied to prompt emission duration).
- "Jet break" observed at $\theta_{ob}\Gamma_{axis} \sim 1$.
- If AG is resolved at the "jet break" moment, it should appear distorted (dislocated) along the projection of the explosion axis on the plane of the sky, with apparent expansion velocities along the axis reaching $\sim 1/\theta_{ob}$; if polarized, position angle should be along the axis
- XRFs and GRBs form a continuous sequence.
- Few orphan AGs.

- Same total kinetic energy in XRF and GRBs, since $E_{\text{tot}} \sim \int d\Omega L_{\Omega} \propto \ln \sin \theta_0$, where $\theta_0 \sim 10^{-3} - 10^{-2}$ is the angular size of the current-carrying core.
- XRFs have on average the same duration as GRBs, determined by the activity period of the central source.

Theoretical implications of the EMM

- Variability of the prompt emission reflects the statistical properties of dissipation (and not the source activity as in the FBM). This is similar to the case of solar flares, which show variability on a wide range of temporal scale unrelated to the time scale of magnetic field generation in tachocline.
- Variability may be enhanced due to random relativistic motion of the "fundamental emitters" in the outflow bulk frame. Highly magnetized medium can support disturbances propagating with high Lorentz factor in the bulk frame; alternatively, magnetic dissipation processes, like reconnection, may produce highly relativistic streams of plasma.
- "Standard candle" - the narrow distribution of GRB energies - may be related to critically rotating relativistic stellar mass object, a one parameter family (under-energetic GRBs may be related to sub-critically rotating central objects)
- Particle acceleration is due to dissipation of magnetic energy (and not shock acceleration as in the FBM). Investigation of magnetic dissipation in the strongly magnetized plasma is only beginning Lyutikov (2003); Zenitani and Hoshino (2004).

The Swift mission, with its early response, should be able to distinguish between FBM and EMM. At a basic level, Lorentz factors in the EMM model are higher, which leads to more energetic early AGs with higher peak frequencies.

References

- Beloborodov, A. M., 2002, ApJ, 565, 808
 Coburn, W., & Boggs, S.E. 2003, Nature , 423, 415
 Daigne, F. and Mochkovitch, R., 2002, MNRAS, 336, 1271-1280
 Heyvaerts, J. and Norman, C., 2003, ApJ, 596, 1240-1255
 Lazzati, D. et al., 2004, astro-ph/0401315
 Lyutikov, M. and Blandford, R., 2003, astro-ph/0312347
 Lyutikov, M., 2003, MNRAS, 346, 540
 Lyutikov, M., Pariev, V., Blandford, R., 2003, ApJ, 597, 998
 McKinney, J. C. and Gammie, C. F., 2004, astro-ph/0404512
 Piran, T., 2004, astro-ph/0405503
 Shapiro, P., 1979, ApJ, 233, 831
 Zenitani, S. and Hoshino, M., 2004, astro-ph/0411373

Zhang, B., Kobayashi, S., 2004, astro-ph/0404140